Ramachandran, L. K., & Witkop, B. (1967) *Methods Enzymol. 11*, 283–295.
Roberts, S. J., Tanner, M. J. A., & Denton, R. M. (1982) *Biochem. J. 205*, 139–145.
Schneider, C., Newman, R. A., Sutherland, R. D., Asser, U., & Greaves, M. F. (1982) *J. Biol. Chem. 257*, 10766–10769.
Shanahan, M. F., Morris, D. P., & Edwards, B. M. (1987) *J. Biol. Chem. 262*, 5978–5984.
Tai, P.-K. K., & Carter-Su, C. (1988) *Biochemistry 27*, 6062–6071.
Thorens, B., Sarkar, H. K., Kaback, H. R., & Lodish, H. F. (1988) *Cell 55*, 281–290.

Differential Scanning Calorimetric Studies of Ethanol Interactions with Distearoylphosphatidylcholine: Transition to the Interdigitated Phase†

Elizabeth S. Rowe* and Terri A. Cutrera

Department of Biochemistry and Molecular Biology, University of Kansas Medical Center, Kansas City, Kansas 66103, and Veterans Administration Medical Center, Kansas City, Missouri 64128

Received March 5, 1990; Revised Manuscript Received August 8, 1990

ABSTRACT: It is well established that ethanol and other amphipathic molecules induce the formation of a fully interdigitated gel phase in saturated like-chain phosphatidylcholines (PC's). We have previously shown that the induction of interdigitation in PC's by ethanol is dependent upon the alcohol concentration, the lipid chain length, and the temperature [Nambi, P., Rowe, E. S., & McIntosh, T. J. (1988) *Biochemistry 27*, 9175–9182]. In the present study, we have used high-sensitivity differential scanning calorimetry to investigate the transitions of distearoylphosphatidylcholine between the noninterdigitated and the interdigitated phases. The enthalpy of the L_{β}' to $L_{\beta}I$ transition is approximately half that of the L_{β}' to P_{β}' transition which occurs in the absence of ethanol. The reversibility of these transitions has also been investigated by employing both heating and cooling scans in order to establish the most stable phases as a function of temperature and ethanol concentration. It has been demonstrated that the transition to the interdigitated phase is reversible as a function of temperature. Kinetic studies on the reverse transition ($L_{\beta}I$ to L_{β}') demonstrate that this transition can be very slow, requiring weeks to reach completion. The rate depends upon temperature and ethanol concentration. The slow phase changes mean that the lipid can exist for long periods of time in a phase structure which is not the most stable state. The biological significance of this type of lipid behavior is the implication that the phase structure of biological membranes may depend not only on the most stable phase structure of the lipids present but also on the synthetic pathway or other kinetic variables.

Interdigitated lipid phases are among the most recently recognized stable phase states for lipids (McDaniel et al., 1983; McIntosh et al., 1983; Ranck et al., 1977; Huang et al., 1983; Slater & Huang, 1988). In 1983, we showed that ethanol had a biphasic effect on the melting temperature of disaturated like-chain phosphatidylcholines (PC's)[1] (Rowe, 1983) which was subsequently shown to be caused by induction of interdigitation in the PC by ethanol (Simon & McIntosh, 1984; Simon et al., 1986). In like-chain PC's, it is induced by a variety of additives including glycerol, methanol, ethylene glycol, benzyl alcohol, chlorpromazine, tetracaine, ethanol, thiocyanate ion (McDaniel et al., 1983; McIntosh et al., 1983; Cunningham & Lis, 1986; Slater & Huang, 1988), and the *n*-alcohols up to heptanol (Rowe & Nelson, 1990). In the absence of additives, dipalmitoylphosphatidylcholine (DPPC) and distearoylphosphatidylcholine (DSPC) go into the interdigitated phase at increased hydrostatic pressure (Braganza & Worcester, 1986; Prasad et al., 1987). The ether analogue of DPPC, dihexadecylphosphatidylcholine (DHPC), exists in the interdigitated state under normal pressures in the absence of any additives (Ruocco et al., 1985; Kim et al., 1987; Laggner et al., 1987), as does 1,3-DPPC (Serrallach et al., 1983). Phosphatidylglycerol (PG) with like chains also goes into the interdigitated phase in the presence of a variety of additives, as well as small proteins such as myelin basic protein and polymyxin (Ranck & Tocanne, 1982; Boggs & Rangaraj, 1985). PG also becomes interdigitated in the presence of Tris buffer (Wilkinson et al., 1987). Mixed-chain PC's also exhibit interdigitated phases if one acyl chain is approximately twice as long as the other (Huang et al., 1983; Hui et al., 1984; Xu & Huang, 1987; Mattai et al., 1987). Lyso-PC's interdigitate (Mattal & Shipley, 1986; Hui & Huang, 1986), and *N*-acylsphingomyelins have recently been shown to exist in a interdigitated state depending upon the length of the variable acyl chain relative to the invariant sphingosine chain (Levin et al., 1985; Maulik et al., 1986). The apparent prevalence of this type of lipid stucture suggests the possibility that it may have some biological relevance.

Most of the research which has been reported regarding the interdigitated phases concerns their structural characterization by X-ray diffraction, and the various methods of detecting the

† This research was supported by the Medical Research Service of the Department of Veterans Affairs and by the National Institute of Alcoholism and Alcohol Abuse (AA-05371).

* Address correspondence to this author at the Veterans Administration Medical Center, 4801 Linwood Blvd., Kansas City, MO 64128.

[1] Abbreviations: PC, phosphatidylcholine; PE, phosphatidylethanolamine; PG, phosphatidylglycerol; DSC, differential scanning calorimetry; DSPC, distearoylphosphatidylcholine; DPPC, dipalmitoylphosphatidylcholine; DHPC, dihexadecylphosphatidylcholine.

presence of interdigitation. In order to elucidate the biological implications of this phase structure, it is necessary to determine its thermodynamic characteristics and the conditions under which this phase occurs. Because of the unusual nature of this phase, an understanding of its thermodynamic properties will contribute to our understanding of the physical chemistry of lipids in general.

In our laboratory, we have been focusing on the alcohol induction of interdigitation in like-chain PC's. In our previous studies, it was shown that the ethanol-induced transition from noninterdigitated L_{β}', to the interdigitated $L_{\beta}I$ phase is dependent on the alcohol concentration, the lipid chain length, and also on temperature (Nambi et al., 1988; Rowe, 1983, 1985; Veiro et al., 1987). The temperature dependence of this transition makes it accessible to investigation by differential scanning calorimetry. In the present investigation, we have used high-sensitivity differential scanning calorimetry (DSC) to investigate the transitions of DSPC between the interdigitated and noninterdigitated phases.

Materials and Methods

Lipid Samples. DSPC was obtained from Sigma or Avanti. The DSPC from these two sources gave similar calorimetric results, but there were some differences; these are noted in the text where appropriate. The samples used for the DSC experiments were hand-shaken multilamellar liposomes prepared essentially by the method of Bangham et al. (1967). Chloroform stock solutions were dried to a film under nitrogen and then kept overnight on a vacuum pump to remove all residual chloroform. Stock suspensions were then hydrated with distilled water by incubation above the melting temperature for at least 1 h with occasional vortexing. Aliquots were removed from the stock suspensions, and ethanol was added accordingly. Unless specified in the text, the ethanol was added at a temperature below the beginning temperature for the experiment at least 1 h prior to the DSC experiment, and the sample was held at this temperature until it was loaded into the calorimeter. In order to avoid any contributions from the subtransition, samples which had been stored in the refrigerator were cycled to at least 30 °C before cooling and addition of ethanol. Lipid concentrations were determined by phosphorus analysis by the method of Bartlett (1957). Analyses were performed on the stock solutions and on each individual calorimetry sample.

Differential Scanning Calorimetry (DSC). DSC was performed by using the MC2 scanning calorimeter with downscanning capability from Microcal, Inc., Amherst, MA. The calorimeter is interfaced with an IBM PS/2 Model 30 computer, and the software used is that provided by Microcal. The temperature decrease for cooling scans is provided by a Haake FC3 refrigerated bath which is controlled by the computer. For heating scans, the scan rate can be varied from 3.75 to 90 °C/h; for our studies of the main transition, the scan rate used was either 4 or 10 °C/h. For the studies of the pretransition or the transition to the interdigitated phase, a heating rate of 60 °C/h was used. In the cooling mode, 5 or 10 °C/h was used for the main transition, and 30 °C/h, the maximum that the bath could provide, was used for the broader transitions. For the very sharp transitions observed in these studies, the transition width was determined from the raw data in order to avoid any distortions due to the interpolation and normalization routines of the Microcal software.

The samples used in this study were suspensions of multilamellar liposomes, which readily settle to the bottom of their vessel. The calorimeter cells were filled as suggested by the manufacturer, and then the sample in the filling tube was removed to avoid a 15–20% error due to settling of the lipid from the filling tube into the calibrated cell volume. It was found that leaving the filling tube mostly empty, i.e., air-filled, did not increase the noise level or precision of the data obtained. For each experiment, the reference cell was filled with water containing the same ethanol concentration as the sample. The lipid concentration in the calorimetry samples was between 0.5 and 6.0 mg/mL lipid.

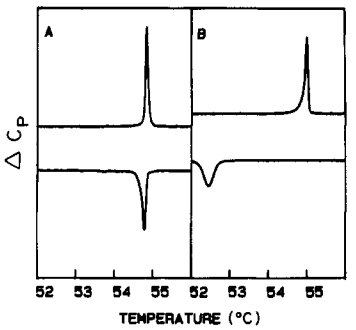

FIGURE 1: DSC traces of raw data for Avanti DSPC for heating (upper trace) and cooling scans. Lipid concentration is 0.65 mg/mL. (A) No ethanol; (B) 50 mg/mL ethanol. The scan rates for heating were 3.75 °C/h and for cooling 4.85 °C/h.

Results

Main Transitions. Figure 1A shows an example of the DSC data obtained on DSPC in water for both heating and cooling scans over the main transition from P_{β}' to L_{α} and reverse. These transitions are very narrow; the width at half-height is 0.06 °C for the heating scan and 0.10 °C for the cooling scan. The data in Figure 1 are for Avanti DSPC; for the Sigma DSPC, the widths was 0.23 °C for the heating scans and 0.35 °C for cooling. There is a difference in the transition temperatures for heating and cooling scans in Figure 1A of 0.1 °C, which is easily detected for the narrow transitions observed with the Avanti DSPC. Because of the difficulty of calibrating the instrument for downscanning, it is likely that this discrepancy arises from the inherent inaccuracy of the instrument calibration. However, it has been suggested recently that the main melting transition of DPPC is not thermodynamically reversible (Tenchov et al., 1989), so the possibility exists that the discrepancy in heating and cooling observed in Figure 1A represents a true discrepancy reflecting irreversibility.

Figure 1B shows the main melting transition of DSPC in the presence of 50 mg/mL ethanol, a concentration at which the lipid is interdigitated prior to melting, so that the observed transition is the $L_{\beta}I$ to L_{α} transition. Similar to that in Figure 1A, this transition is very narrow for the heating scan (0.09 °C width at half-height) but is broader for the cooling scan (0.4 °C width at half-height). For the Sigma lipid, the transitions were again broader than those of the Avanti lipid. As reported previously for DPPC (Rowe, 1985), there is a large hysteresis in this transition; for this concentration of ethanol, there is a difference of nearly 3 °C between main transition temperatures for heating and cooling.

The effect of ethanol on the transition temperature, enthalpy, and the transition hysteresis was investigated by DSC for both transitions, in order to compare the interdigitated phase with the noninterdigitated phase. The main transition temperatures for heating and cooling for the P_{β}' to L_{α} and the $L_{\beta}I$ to L_{α} transitions are plotted in Figure 2 as a function of ethanol concentration. The determination of which transition is being observed was made based on the characteristics of the lower temperature transitions as presented below. The results shown here from DSC are similar to our previously reported

Table I: Transition Enthalpies for the Indicated Transitions for both Avanti and Sigma DSPC[a]

		ΔH (kcal/mol)				
lipid	[ethanol] (mg/mL)	$L_{\beta'}$ to $P_{\beta'}$	$L_{\beta'}$ to $L_\beta I$	$P_{\beta'}$ to L_α	$L_\beta I$ to L_α	total $L_{\beta'}$ to I_α
Avanti DSPC	0	1.55		10.0		11.5
	50		0.750		11.0	11.8
Sigma DSPC	0	1.77		11.2		13.0
	50		0.960		12.0	13.0

[a] Each value is an average of many measurements. The standard deviation for the main transitions is 0.7 kcal/mol.

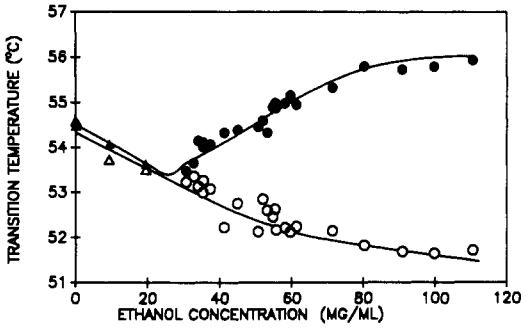

FIGURE 2: Transition temperatures for the "main" transitions as a function of ethanol concentration for heating and cooling scans. Triangles represent the $L_{\beta'}$ to $P_{\beta'}$ transition; circles represent the $L_{\beta'}$ to $L_\beta I$ transition. Filled symbols represent heating scans; open symbols represent cooling scans.

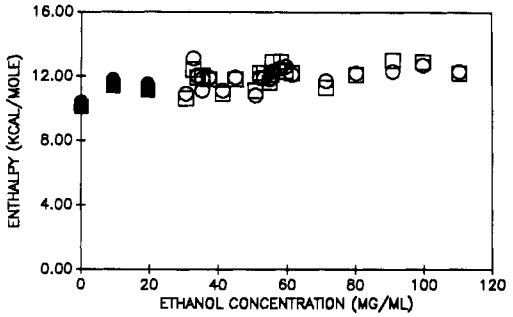

FIGURE 3: Main transition enthalpy for Sigma DSPC in kilocalories per mole. Filled symbols represent the $P_{\beta'}$ to L_α transition; open symbols represent the $L_\beta I$ to L_α transition. Circles represent data from heating scans; squares represent data from cooling scans.

results using other methods (Rowe, 1983, 1985). This figure shows that for the $P_{\beta'}$ to L_α transition the transition temperature is decreased as a function of ethanol concentration and the transition hysteresis remains small. In contrast, for the $L_\beta I$ to L_α transition, there is an increase in transition temperature for the heating scans, and a progressively greater hysteresis as a function of ethanol concentration.

Figure 3 shows a plot of the enthalpy of the main transition as a function of ethanol concentration, with different symbols representing the $L_\beta I$ to L_α transition and the $P_{\beta'}$ to L_α transition. These data can be fit to a straight line with a slightly positive slope. However, since we know that the phase change being observed is different above and below 25 mg/mL ethanol, we have instead analyzed the two regions separately. This analysis gives an enthalpy for the $L_\beta I$ to L_α transition of 12.0 kcal/mol (standard deviation 0.7) and for the $P_{\beta'}$ to L_α transition of 11.2 kcal/mol (standard deviation 0.6). These two values are nearly within experimental error of each other. The results given in Figure 3 are on DSPC from Sigma; the enthalpies for the Avanti lipid were systematically lower by approximately 10%. The reason for this difference is not understood. The enthalpies are summaried in Table I for the Sigma and Avanti lipids.

The I Transition and the Pretransition. Figure 4 shows DSC scans of the low-temperature transition of DSPC as a

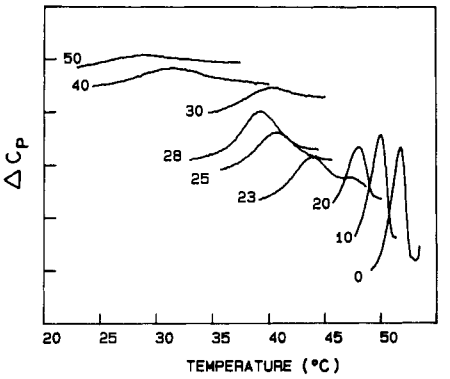

FIGURE 4: DSC scans of lower temeprature transition as a function of ethanol concentration. Figures on the plot represent the concentration of ethanol in milligrams per milliliter. Lipid concentration is 5.5 mg/mL Avanti DSPC.

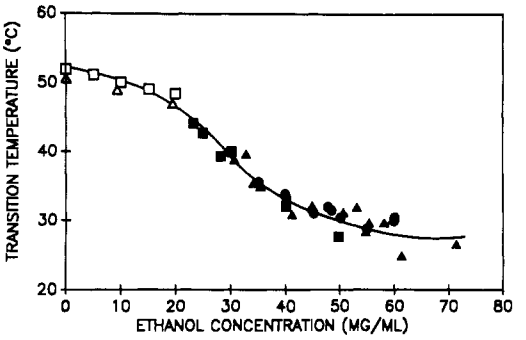

FIGURE 5: Transition temperatures from heating scans for the pretransition ($L_{\beta'}$ to $P_{\beta'}$) and the I transition ($L_{\beta'}$ to $L_\beta I$). Open symbols represent pretransitions; filled symbols represent I transitions. The determination of which transition was being observed was made by evaluation of the transition shape as shown in Figure 4. Squares represent Avanti lipid; circles and triangles represent Sigma lipid.

function of ethanol concentration. For convenience, the $L_{\beta'}$ to $L_\beta I$ transition is referred to as the I transition, and the $L_{\beta'}$ to $P_{\beta'}$ transition is referred to as the pretransition. The temperature of the pretransition moves to lower temperature as the ethanol concentration is increased, in agreement with our earlier optical density data (Veiro et al., 1987). Between 20 and 25 mg/mL ethanol, there is a discontinuous change in the shape of the observed transition, corresponding to the disappearance of the pretransition as observed by optical density (Veiro et al., 1987) and the appearance of the I transition as observed by fluorescence (Nambi et al., 1988). The temperature of the I transition continues to decrease with ethanol concentration, also becoming broader with concentration.

Figure 5 shows the temperature of the pretransition and the I transition as a function of ethanol concentration. The two transitions were distinguished by the shapes of the DSC scans in Figure 4, and are denoted by different symbols. Data from both Avanti and Sigma DSPC are included. This plot is superimposable with the data obtained by fluorescence (Nambi et al., 1988), except that no data were obtained above 70 mg/mL ethanol. The lack of an observable transition by DSC

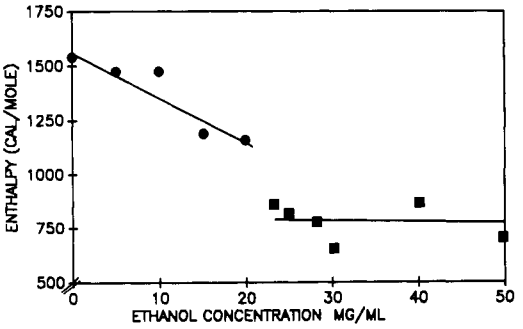

FIGURE 6: Enthalpy for the pretransition and the I transition as a function of ethanol concentration, measured on Avanti DSPC. Circles represent the pretransition (L_β' to P_β'); squares represent the I (L_β' to $L_\beta I$) transition. The determination of which transition was being observed was made by evaluation of the transition shapes.

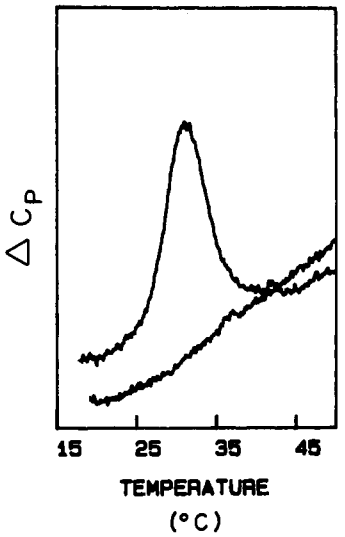

FIGURE 7: First and immediate second heating scans of DSPC in the presence of 45 mg/mL ethanol. The scan rate was 60 °C/h; the lipid concentration was 4.0 mg/mL.

above 70 mg/mL ethanol is due to the fact that the lipid becomes interdigitated at this concentration during the time required to equilibrate the instrument prior to the scan. This is consistent with the kinetic data presented below.

Figure 6 shows a plot of the enthalpy of the pretransition and the I transition as a function of ethanol concentration for the Avanti DSPC. Unlike the main transition, the pretransition exhibits a decrease in enthalpy with increasing alcohol concentration. In contrast, the enthalpy of the I transition remains fairly constant as a function of ethanol concentration up to 50 mg/mL ethanol; above this concentration, it drops slightly. The enthalpies for the pretransition and the I transitions for both the Avanti and Sigma DSPC's are summarized in Table I. As seen here, the enthalpy for the I transition is approximately half that for the pretransition for both lipids.

Reversibility of the I Transition. Figure 7 shows an initial heating scan exhibiting an I transition for a DSPC sample containing 45 mg/mL ethanol. A subsequent cooling scan showed no transition. The second heating scan immediately after the cooling scan, shown in Figure 7, exhibits no I transition. However, after incubation in the calorimeter for 2 days at 15 °C, a third heating scan exhibits an I transition in its original intensity. Thus, it can be concluded that the transition is reversible but that it is quite slow. In order to further characterize the reversibility of this transition and to determine what the thermodynamically most stable state is under various conditions, a series of kinetic experiments were performed. For most of the experiments, the temperature selected for the study

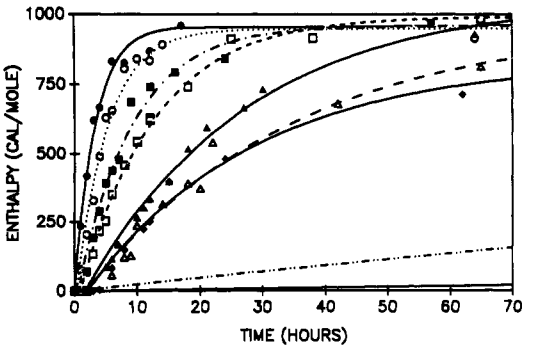

FIGURE 8: Recovered enthalpy in calories per mole of I transitions as a function of time of incubation at 15 °C, for several ethanol concentrations. The lines through the points represent first-order rate functions, fitted to the data by nonlinear least-squares analysis. From left to right, the ethanol concentrations are (solid circles) 35, (open circles) 40, (solid squares) 45, (open squares) 47.9, (solid triangles) 48.5, and (open triangles) 50 mg/mL. The lower two lines represent theoretical first-order functions based on one or two very long time points at 55 mg/mL ethanol and 60 mg/mL ethanol, as described in the text.

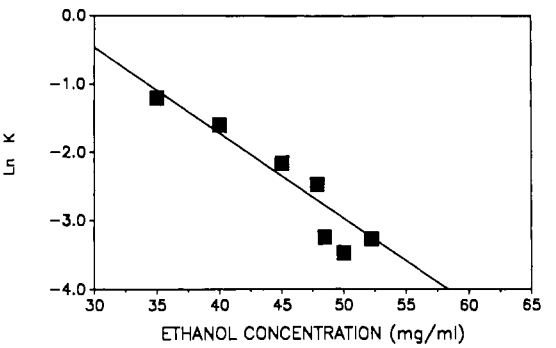

FIGURE 9: Rate constants for recovery of the I transition at 15 °C as a function of ethanol concentration.

of the reverse I ($L_\beta I$ to L_β') transition was 15 °C. This temperature was chosen because it was sufficiently far from the transition in the heating direction to expect significant reversal, and yet it was not low enough to lead to interference from the subtransition.

The recovery of the noninterdigitated L_β' phase was investigated by heating and cooling the sample in the calorimeter, and then holding it in the calorimeter at 15 °C for a selected length of time. A heating scan was then performed and the enthalpy of the observed I transition measured. The observed enthalpy was considered to represent the amount of the lipid that had recovered the L_β' phase during the selected time interval and thus was able to undergo the temperature-induced transition to the $L_\beta I$ phase again.

Figure 8 shows a plot of the recovered enthalpy of the I transition against time for a series of ethanol concentrations. The lines represent nonlinear least-squares fits of these data to first-order equations. At each ethanol concentration studied, the data fit a first-order equation well, suggesting that the process of the transition approximates a first-order mechanism. The nonlinear least-squares method of fitting allows the infinite time enthalpy and the zero time enthalpy to be fitting parameters. We found that the time infinity values agreed well with the enthalpies measured in the initial scans up to 52 mg/mL ethanol. The zero time value was consistently negative, usually −70 cal/mol. In addition, there was clearly a time lag before the first observable recovery appeared in the higher alcohol experiments. These observations suggest that there may be a preequilibration or nucleation process which occurs prior to the apparently first-order process which gives

rise to a recovered L_{β}' phase detected by the recovered I transition.

The rate constants obtained in the data fitting are plotted in Figure 9 against ethanol concentration. The dependence of this log plot on ethanol concentration appears to be linear. Extrapolation of this line to zero ethanol concentration gives a rate constant of 30/h, which gives a half-time of 1.4 min.

Above 52 mg/mL ethanol, there is an abrupt drop in the rate of recovery. The two lower lines on the plot of Figure 8 represent experiments at 55 and 60 mg/mL ethanol in which only one or two points were measured and a rate equation was determined based on an assumed final value. For 55 mg/mL ethanol, the first point at 118 h gave an enthalpy of 250 cal. For 60 mg/mL ethanol, a barely detectible peak of 80 cal/mol was observed after 12 days at 15 °C. The apparent lack of recovery at 60 mg/mL ethanol raised the possibility that at this ethanol concentration the most stable phase was the interdigitated phase. This was tested by preparing an identical sample with 60 mg/mL ethanol and keeping it at 15 °C for 12 days prior to the first heating. It was found that upon heating this sample gave a strong I transition with an enthalpy of 794 cal/mol, which compares favorably with the enthalpy of 733 cal/mol measured in the initial scan of the parallel sample 1 h after ethanol addition. From these two experiments, we conclude that it cannot be determined which phase is the most stable at 15 °C, since no change occurred in either of the two samples for 12 days at the same temperature and ethanol concentration. At 70 mg/mL ethanol, the I transition began to disappear upon incubation of 6 h prior to the first scan, suggesting that at 70 mg/mL ethanol and 15 °C the interdigitated phase may be the more stable.

In addition to the extensive temperature reversal experiments described above, several solvent dilution experiments were performed. The purpose was to determine whether a sample of interdigitated lipid would recover the properties appropriate for the lower ethanol concentration after dilution. In a typical experiment, the lipid was heated and cooled in the presence of 90 mg/mL ethanol so that it was interdigitated. The sample was then diluted to approximately 13 mg/mL ethanol and scanned within 2 h. The heating scan was identical with that obtained from a 13 mg/mL ethanol sample which had not been previously interdigitated, exhibiting a typical pretransition at the expected temperature. These results suggest that the reversal of interdigitation per se is not particularly slow after the ethanol has been removed. Extrapolation of the plot in Figure 9 to 13 mg/mL ethanol gives a rate constant of 5.5/h which corresponds to a half-time of 7.5 min. This is consistent with our observation that the recovery is rapid after dilution of the ethanol.

The temperature dependence of the recovery kinetics was investigated by measuring the recovery at 40 mg/mL ethanol at several temperatures ranging from 15 to 22 °C. Data were collected at 12 °C, but the appearance of the subtransition interfered with accurate measurements of the smaller I transition enthalpy. The temperature dependence of the rate constants give rise to an activation energy of 51 cal/mol.

Conditions of Stability for $L_{\beta}I$. The data from the heating scans and the recovery data have been combined to delineate the conditions of stability for each of the phases; these data are summarized in Figure 10. The open diamonds represent temperature dependence experiments similar to those described above, performed in order to determine the highest temperature at which detectable recovery was obtained in 18 h, for each ethanol concentration. The line connecting these points represents the highest temperatures and ethanol concentrations

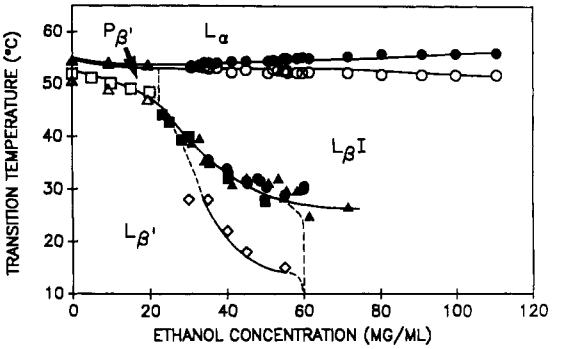

FIGURE 10: Summary of the conditions of stability of DSPC phases as a function of temperature and ethanol concentration. Data points are from Figures 2 and 5 and represent the midpoints of the respective transitions. The open diamonds represent the highest temperature where significant reversal of the L_{β}' to $L_{\beta}I$ transition occurred in 18 h at each concentration. The region between the solid line (L_{β}' to $L_{\beta}I$ transition temperatures) and the open diamonds (slow recovery of L_{β}' via the $L_{\beta}I$ to L_{β}' transition) represents the conditions in which the phase state of the lipid depends not only on temperature and ethanol concentration but also on sample history. The vertical dashed line between the P_{β} and $L_{\beta}I$ regions connects the observed triple point on the lower line with the inflection point of the main transition curve on the upper line.

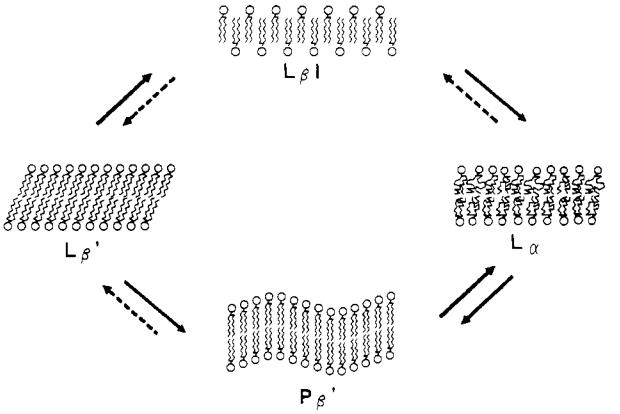

FIGURE 11: Illustration of the phase structures of DSPC, with temeprature increasing from left to right. The upper pathway occurs in the presence of sufficient ethanol; the lower pathway occurs in the absence of ethanol or at low ethanol concentration. The dashed arrows represent phase changes which are slow or which exhibit hysteresis on a macroscopic time scale.

at which the L_{β}' phase is the most stable phase. The line connecting the apparent L_{β}' to $L_{\beta}I$ transition temperatures from heating scans represents the lowest temperatures at which the $L_{\beta}I$ phase is the most stable. The large region between these lines represents those conditions where metastable phases occur, and the phase which exists depends upon the sample history.

Also shown in Figure 10 are the main transition data. As we have previously discussed (Rowe, 1985), there is a region of metastability also between the heating and cooling curves for the $L_{\beta}I$ to L_{α} transition. The dashed line between the P_{β}' and the $L_{\beta}I$ regions of the diagram connects the P_{β}'–L_{β}'–$L_{\beta}I$ triple point on the lower curve with the approximate point of inflection of the main transition melting temperature curve.

Discussion

Figure 11 shows an illustration of the phase structures and transitions which occur in the range of conditions explored in this investigation. The crystalline subgel phase is not pictured because we have carefully avoided those conditions under which it occurs. As illustrated here, temperature is increasing

from left to right. The upper pathway represents the sequence of phase structures that occur in the presence of ethanol above 25 mg/mL as the lipid is heated through the I and then the main transition. The lower pathway represents that taken in the absence of ethanol and below 20 mg/mL ethanol for DSPC. We have measured the enthalpy of each of the processes illustrated here.

The transition from $L_{\beta'}$ to $L_{\beta}I$, also known as the I transition, has been explored in detail in this investigation. The transition would appear to involve a relatively major structural rearrangement, as illustrated in Figure 11, yet the enthalpy change of the transition is small, particularly when compared to the parallel $L_{\beta'}$ to $P_{\beta'}$ transition, known as the pretransition, which occurs in the absence of ethanol. This suggests that there must be some compensatory mechanisms taking place in this complex transition.

The low enthalpy of the I transition relative to the pretransition indicates that from the point of view of enthalpy alone, the I transition would not be favored over the pretransition. The origin of the low enthalpy of the I transition may be understood by considering the regions of the bilayer separately. For example, in the head-group region, there is an increase in area per head group during the I transition. This process is analogous to that which occurs to a lesser degree in the pretransition. It may be expected to make a negative enthalpy contribution to the process because of the reduction in head-group interactions, particularly steric crowding. However, in the acyl chain region, there is an *increase* in density and in the van der Waals contacts (Simon & McIntosh, 1984) in the I transition which may be expected to make a positive enthalpy contribution. This suggests that the observed enthalpy of the I transition may contain contributions from a negative enthalpy change due to the head-group region and a positive enthalpy change in the acyl chain region.

By comparison, in the parallel $L_{\beta'}$ to $P_{\beta'}$ transition in the absence of ethanol, there is a *reduction* in acyl chain packing (Janiak et al., 1976; Stamatoff et al., 1982) which would be expected to make a negative enthalpy contribution. This transition has an increase in head-group area which is less than that occurring in the I transition; this would also make a negative enthalpy contribution. Again, since the contributions from the two regions are additive, for the pretransition the contributions from the head-group region and from the acyl chain region would be of the same sign. Thus, by comparison of the pretransition and the I transition, it is suggested that the lower enthalpy of the I transition is due in part to a positive enthalpy contribution from the increased van der Waals packing which occurs in the acyl chain region in the I transition.

The free energy differences between the $L_{\beta'}$ and $L_{\beta}I$ phases have been discussed by Simon et al. (1986). They suggest that the dominating forces in comparing $L_{\beta'}$ with $L_{\beta}I$ are the favorable energy contributed by the increase in van der Waals interactions in the acyl chain region and the unfavorable energy contributed by the increase in area per head group leading to exposure of the terminal methyls to the solvent. They did not discuss the $P_{\beta'}$ phase. From this perspective, it is clear that the source of the free energy which stabilizes $L_{\beta}I$ over $L_{\beta'}$ and over $P_{\beta'}$ is the effect of ethanol (or other inducer) in reducing the unfavorable interactions of the terminal methyls with the solvent interface which occurs with the increase in area per head group. This would be expected to be a largely entropic effect because it is apparently largely hydrophobic (Tanford, 1980). Simon et al. do not consider any contribution for the change in area per head group other than this exposure of hydrophobic groups. However, we have previously provided evidence that phosphatidylethanolamines (PE's) do not interdigitate in the presence of ethanol (Rowe, 1985) and do not participate significantly in interdigitation in binary mixtures with interdigitated PC (Rowe, 1987). The PE head group is smaller than the cross-sectional area of the acyl chains and thus does not cause crowding in the gel phase. This suggests that another favorable source of energy for interdigitation in PC's would be the stearic crowding of the PC head groups in the $L_{\beta'}$ phase, which destabilizes this phase and gives rise to the $P_{\beta'}$ phase in the absence of ethanol and the $L_{\beta}I$ phase when a sufficient concentration of amphipathic inducer such as ethanol is present. We have also shown previously that the choline methyls of DPPC have more mobility in the $L_{\beta}I$ phase than in the $P_{\beta'}$ phase (Herold et al., 1987), also suggesting that head-group crowding may favor $L_{\beta}I$ over $P_{\beta'}$.

As shown in Table I, the total enthalpy in going from $L_{\beta'}$ to L_{α} is the same within experimental error regardless of which of the pathways in Figure 11 is followed; the main transition $L_{\beta}I$ to L_{α} has a slightly larger enthalpy than the $P_{\beta'}$ to L_{α} transition which compensates for the lower enthalpy of the $L_{\beta'}$ to $L_{\beta}I$ compared to $L_{\beta'}$ to $P_{\beta'}$ discussed above. This is as expected if Figure 11 represents the correct total of the processes involved. What is not included in these calculations is any structural effect of ethanol on the L_{α} or $L_{\beta'}$ phases. At the present time, there is no evidence to suggest that the structure of the $L_{\beta'}$ phase or the L_{α} phase is altered by the presence of ethanol. However, ethanol binding could contribute to the observed total enthalpy if there is a significant difference in ethanol binding between the $L_{\beta'}$ phase and the L_{α} phase, and if this binding involves significant enthalpy effects. The lack of a significant difference in the observed total enthalpy change between $L_{\beta'}$ and L_{α} in the presence and absence of ethanol does not rule out differences in ethanol binding because such binding would not necessarily involve significant enthalpy changes.

Reversibility of Interdigitation. The reversibility studies as a function of temperature and ethanol concentration demonstrate the reversibility of the transition from the noninterdigitated $L_{\beta'}$ phase to the interdigitated $L_{\beta}I$ phase. This is very important because without the demonstration of reversibility, no information about the relative stabilities of the different phases can be obtained. For example, it could not be ruled out that the observed transition upon heating was a kinetic phenomenon only and that once the lipid became interdigitated it would remain interdigitated at all temperatures below the main melting transition.

The summary of phase behavior in Figure 10 shows two regions of metastability, the one between the $L_{\beta}I$ and L_{α} phases, elucidated previously (Rowe, 1985), and the one investigated in the present study between the $L_{\beta'}$ and $L_{\beta}I$ phases. Under these conditions, the phase of the lipid depends not only on the temperature and ethanol concentration but also on time and the sample history. The true equilibrium point between the phases must be somewhere within this region, but it cannot be determined experimentally. One consequence of the regions of metastability involving the $L_{\beta}I$ phase is that the observed transitions between these phases are not equilibrium transitions. For this reason, the transition curves such as shown in Figures 1 and 4 cannot be analyzed by strict thermodynamic theories to determine the van't Hoff enthalpy and the cooperaive unit size etc.

An outstanding characteristic of the transitions between the $L_{\beta'}$ and $L_{\beta}I$ phases is that they are very slow, particularly the $L_{\beta}I$ to $L_{\beta'}$ transition. The reasons for the slowness of this

process are not apparent. Although the multilamellar vesicle system may introduce kinetic barriers due to the need for mass transport of solvent, for example, when there is a change in bilayer spacing, this would not appear to be sufficient to explain the slow kinetics, since the kinetics are not particularly slow when the ethanol is removed by dilution. There is ample precedent for lipid phase behavior to involve slow transitions and metastable states. Our results demonstrate that the fully interdigitated phase of saturated PC's, in the presence of ethanol, is among those phases which are highly ordered and do not rapidly equilibrate, and are thus not necessarily in their most stable phase under any given conditions. The biological implication of this observation is that the phase structures of membrane lipids in vivo may not necessarily be determined thermodynamically by the conditions and by the lipid composition, but they could be determined also by the pathway of synthesis or other kinetic variables.

The biological significance of interdigitation is not yet known. However, if it occurs in biological membranes, it could have important functional consequences, which have been discussed by Slater and Huang (1988). The interdigitation of lipids has some features which are different from any of the other identified phases accessible to lipids. For example, it provides a means of coupling the two sides of the bilayer, which are uncoupled in the classical bilayer. It also changes the bilayer thickness, which could provide a mechanism of regulation of membrane proteins. It reduces the surface charge density, which may be important in membrane fusion. Finally, it results in the loss of the bilayer midplane, a particularly fluid region of the bilayer, which could trigger conformational changes in membrane proteins. Although interdigitated phases have not yet been directly detected in biological membranes, the wide variety of lipids which can participate in this type of structure and the small energy difference between interdigitated and noninterdigitated phases suggest that they may occur in biological membranes.

References

Bangham, A. D., DrGier, J., & Greville, G. D. (1967) *Chem. Phys. Lipids 1*, 115–145.

Bartlett, G. R. (1957) *J. Biol. Chem. 234*, 466.

Boggs, J. J. M., & Rangaraj, G. (1985) *Biochim. Biophys. Acta 816*, 221–233.

Boggs, J. M., & Mason, J. T. (1986) *Biochim. Biophys. Acta 863*, 231–242.

Braganza, L. F., & Worcester, D. L. (1986) *Biochemistry 25*, 2591–2596.

Cunningham, B. A., & Lis, L. J. (1986) *Biochim. Biophys. Acta 861*, 237–242.

Herold, L. L., Rowe, E. S., & Khalifah, R. G. (1987) *Chem. Phys. Lipids 43*, 215–226.

Huang, C., Mason, J. T., & Levin, I. W. (1983) *Biochemistry 22*, 2775–2780.

Hui, S. W., & Huang, C.-H. (1986) *Biochemistry 25*, 1330–1335.

Hui, S. W., Mason, J. T., & Huang, C. (1984) *Biochemistry 23*, 5570–5577.

Janiak, M. J., Small, D. M., & Shipley, G. G. (1976) *Biochemistry 15*, 4575–4580.

Janiak, M. J., Small, D. M., & Shipley, G. G. (1979) *J. Biol. Chem. 54*, 6068–6078.

Kim, J. T., Mattai, J., & Shipley, G. g. (1987) *Biochemistry 26*, 6592–6598.

Laggner, P., Lohner, K., Degovics, G., Muller, K., & Schuster, A. (1987) *Chem. Phys. Lipids 44*, 31–60.

Levin, I., Thompson, T. E., Barenholz, Y., & Huang, C. (1985) *Biochemistry 24*, 6282–6286.

Mattai, J., & Shipley, G. G. (1986) *Biochim. Biophys. Acta 859*, 257–265.

Mattai, J., Sripada, P. K., & Shipley, G. G. (1987) *Biochemistry 26*, 3287–3297.

Maulik, P. R., Atkinson, D., & Shipley, G. G. (1986) *Biophys. J. 50*, 1071–1077.

McDaniel, R. V., McIntosh, T. J., & Simon, S. A. (1983) *Biochim. Biophys. Acta 731*, 97–108.

McIntosh, T. J., McDaniel, R. V., & Simon, S. A. (1983) *Biochim. Biophys. Acta 731*, 109–114.

McIntosh, T. J., Simon, S. A., Ellington, J. C., & Porter, N. A. (1984) *Biochemistry 23*, 4038–4044.

Nambi, P., Rowe, E. S., & McIntosh, T. J. (1988) *Biochemistry 27*, 9175–9182.

Prasad, S. K., Shashidar, R., Gaber, B. P., & Chandrasekhar, S. C. (1987) *Chem. Phys. Lipids 143*, 227–235.

Ranck, J. L., & Tocanne, J. F. (1982) *FEBS Lett. 143*, 171–174.

Ranck, J. L., Keira, R., & Luzzati, V. (1977) *Biochim. Biophys. Acta 488*, 432–441.

Rowe, E. S. (1983) *Biochemistry 22*, 3299–3305.

Rowe, E. S. (1985) *Biochim. Biophys. Acta 813*, 321–330.

Rowe, E. S. (1987) *Biochemistry 26*, 46–51.

Rowe, E. S., & Nelson, J. N. (1990) *Biophys. J. 57*, 474a.

Ruocco, M. J., Siminovitch, D. J., & Griffin, R. G. (1985) *Biochemistry 24*, 2406–2411.

Serrallach, E. N., Dijkman, R., De Haas, G. H., & Shipley, G. G. (1983) *J. Mol. Biol. 170*, 155–174.

Simon, S. A., & McIntosh, T. J. (1984) *Biochim. Biophys. Acta 773*, 169–172.

Simon, S. A., McIntosh, T. J., & Hines, M. L. (1986) *Molecular and Cellular Mechanisms of Anesthetics* (Roth, S. H., & Miller, K. W., Eds.) pp 279–318, Plenum, New York.

Slater, J. L., & Huang, C. (1989) *Prog. Lipid Res. 27*, 325–359.

Stamatoff, J., Feuer, B., Guggenheim, H. J., Tellez, G., & Yamane, T. (1982) *Biophys. J. 38*, 217–226.

Tanford, C. (1980) *The Hydrophobic Effect*, 2nd ed., Wiley, New York.

Tenchov, B. G., Yao, H., & Hatta, I. (1989) *Biophys. J. 56*, 757–768.

Veiro, J. A., Nambi, P., Herold, L. L., & Rowe, E. S. (1987) *Biochim. Biophys. Acta 900*, 230–238.

Weber, G. (1981) *J. Phys. Chem. 85*, 949.

Wilkinson, D. A., Tirrell, D. A., Turek, A. B., & McIntosh, T. J. (1987) *Biochim. Biophys. Acta 905*, 447–453.

Xu, H., & Huang, C.-H. (1987) *Biochemistry 26*, 1036–1043.